ACS Medicinal Chemistry Letters

Letter

Potent, selective and CNS-penetrant tetrasubstituted cyclopropane class IIa histone deacetylase (HDAC) inhibitors

Christopher Andrew Luckhurst, Perla Breccia, Andrew J Stott, Omar Aziz, Helen L Birch, Roland Burli, Samantha J Hughes, Rebecca E Jarvis, Marieke Lamers, Philip M Leonard, Kim L Matthews, George McAllister, Scott Pollack, Elizabeth Saville-Stones, Grant Wishart, Dawn Yates, and Celia Dominguez

ACS Med. Chem. Lett., **Just Accepted Manuscript** • DOI: 10.1021/acsmedchemlett.5b00302 • Publication Date (Web): 10 Dec 2015

ACS Publications

ACS Medicinal Chemistry Letters is published by the American Chemical Society. 1155 Sixteenth Street N.W., Washington, DC 20036

Potent, selective and CNS-penetrant tetrasubstituted cyclopropane class IIa histone deacetylase (HDAC) inhibitors

Christopher A. Luckhurst;† Perla Breccia;† Andrew J. Stott;† Omar Aziz;† Helen L. Birch;† Roland W. Bürli;† Samantha J. Hughes;† Rebecca E. Jarvis;† Marieke Lamers;† Philip M. Leonard;† Kim L. Matthews;† George McAllister;† Scott Pollack;† Elizabeth Saville-Stones;† Grant Wishart;† Dawn Yates;† Celia Dominguez.*,‡

†BioFocus, Charles River, Chesterford Research Park, Saffron Walden, Essex, CB10 1XL, United Kingdom

‡CHDI Management/CHDI Foundation Inc., 6080 Center Drive, Suite 100, Los Angeles, California 90045, United States

KEYWORDS: Class IIa HDAC inhibitors; hydroxamic acid; CNS exposure; tetrasubstituted cyclopropane; cyclopropanation, Huntington 's disease.

ABSTRACT: Potent and selective class IIa HDAC tetrasubstituted cyclopropane hydroxamic acid inhibitors were identified with high oral bioavailability that exhibited good brain and muscle exposure. Compound **14** displayed suitable properties for assessment of the impact of class IIa HDAC catalytic site inhibition in preclinical disease models.

Inhibition of class IIa HDAC enzymes has been suggested as a therapeutic strategy for a number of indications, including Huntington's disease (HD) and muscular atrophy. Class IIa HDACs are large proteins with multiple functions including transcription factor binding and *N*-acetyl lysine recognition.[1,2] Of most interest to our laboratory is the role of class IIa HDAC biology in HD, in particular the beneficial effect which has been observed following HDAC4 genetic suppression.[3-5] Replication of these effects in preclinical models of HD *via* occupancy of the class IIa HDAC catalytic domain would provide a rationale for small molecule therapy. Currently there are no marketed HDAC class IIa-selective inhibitors, whereas four pan-HDAC inhibitors, vorinostat (SAHA), romidepsin, belinostat and panobinostat are on the market.

Class IIa-selective HDAC inhibitors would represent important tools for elucidating the therapeutic potential of this protein family. We recently reported the structure-based design of trisubstituted cyclopropane class IIa-selective HDAC inhibitors as potential therapeutics in HD.[6] This improved selectivity was driven by exploiting a selectivity pocket (**Figure 1**, shown with compound **13**) that is not present in the class I HDAC isoforms. This pocket is formed as a consequence of a tyrosine-histidine substitution.[7]

We now report the discovery of tetrasubstituted cyclopropane hydroxamic acid class IIa HDAC inhibitors, with additional substitution at C1 (**Figure 1**). These compounds exhibited improved pharmacokinetic profiles, and so may provide a further means for evaluating efficacy in preclinical *in vivo* HD disease models.

Determination of the biochemical and Jurkat E6.1 cell potencies of compounds against the HDAC isoforms has been described previously, employing artificial substrates Boc-Lys(TFA)-AMC (class IIa/HDAC8-specific) and Boc-Lys(Ac)-AMC (class I/IIb-specific).[6-10] The majority of class IIa HDAC activity in the Jurkat E6.1 cell line is derived from HDAC4.[6] Biochemical HDAC isoform selectivity was compared to the difference in activity in the cell assays between the Lys-Ac (class I/IIb-specific) and the Lys-TFA (class IIa/HDAC8-specific) substrates.

Figure 1. X-ray structure of HDAC4cd (class IIa HDAC) with trisubstituted cyclopropane 13 (4CBT)[6] showing the presence of a selectivity pocket due to a Tyr-His substitution. Residue numbering from PDB files.

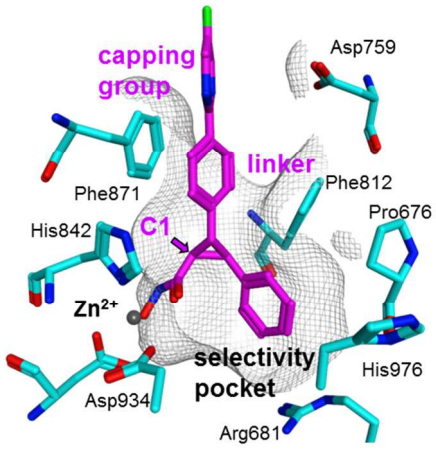

In the trisubstituted cyclopropane series reported previously, the most potent compounds in the biochemical and cell assays, albeit with a significant drop-off in cell potency, had comprised either pyrimidine or oxazole capping groups.[6] Further improvements in biochemical potency and pharmacokinetics were targeted. The design of these molecules was inspired by the expectation that a fluorine atom alpha to the hydroxamic acids may increase their acidity. It has previously been proposed that fluorination of known HDAC inhibitors at the carbon bearing the hydroxamic acid moiety enhanced HDAC biochemical activity.[11] Analysis of the X-ray structures of the trisubstituted cyclopropanes, and docking studies for the new tetrasubstituted cores indicated that there was sufficient space for small substituents to be accommodated at the C1-cyclopropane position.

Trisubstituted cyclopropane hydroxamic acids previously profiled in mouse hepatocytes displayed high intrinsic clearance values.[6] It was assumed that direct glucuronidation would be their principal route of clearance, presumably *via O*-glucuronidation of the hydroxamic acid, and that the contribution of oxidative metabolism to the overall clearance of these molecules would be small. Compounds with very short half-lives (< 5 min) in mouse liver microsomes were not progressed. Substitution of the cyclopropane carbon atom bearing the hydroxamic acid moiety (C1), with either a methyl group or a halogen might limit, either *via* steric or electronic means, the glucuronidation process. Some of the previously reported trisubstituted cyclopropanes had demonstrated high passive permeability and low P-gp efflux in MDR1-MDCK monolayers. We anticipated that reduced clearance, whilst maintaining high passive permeability and low P-gp efflux, would lead to higher plasma and CNS exposures. The C1-substituent on the cyclopropane ring was selected to maintain the favorable CNS-compliant physicochemical properties of the compounds.

Table 1. Impact of cyclopropane substitution alpha to the hydroxamic acid upon potency and *in vitro* ADME properties.

Entry	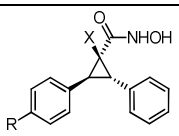		HDAC4 IC_{50} (μM)[a]	Cell Lys(TFA) IC_{50} (μM)[a]	Kinetic solubility (μM)	Cl_{int} (mL/min/kg body weight)[b] liver microsomes		MDCK-MDR1	
	R	X				mouse	human	P_{app} (nm/s)	EER[c]
9	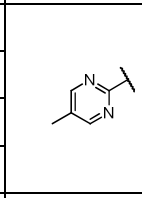	H	0.18±0.09	0.51±0.16	170	>1297	ND	375	2.0
10		Me	0.05±0.01	0.73±0.13	150	281	<36	391	2.0
11		Cl	0.11±0.03	1.15±0.28	140	ND	ND	ND	ND
12		F	0.02±0.006	0.13±0.05	160	570	37	369	2.0
13		H	0.05±0.02	0.33±0.08	45	688	42	294	1.4
14		F	0.01±0.001	0.12±0.03	35	306	<36	418	1.4
15	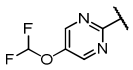	H	0.15±0.02	0.55±0.02	120	73	<36	129	2.2
16		F	0.03±0.01	0.15±0.04	100	<65	<36	192	1.3
17	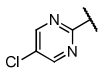	H	0.14±0.03	0.43±0.09	<5	<65	<36	380	2.8
18		F	0.04±0.006	0.23±0.005	<5	73	<36	<10[d]	ND[d]
19	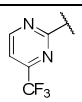	H	0.08±0.04	0.68±0.20	45	>1297	<36	114	2.1
20		F	0.04±0.009	0.28±0.10	55	258	56	70	2.0
21		H	0.03±0.01	0.23±0.06	140	89	<36	442	2.4
22		F	0.01±0.001	0.12±0.03	65	<67	ND	487	1.3

[a] Arithmetic mean and standard error of ≥3 measurements.

[b] Intrinsic clearance (Cl_{int}) values of > 257 mL/min/kg in mouse liver microsomes (MLM) and > 52 mL/min/kg for human liver microsomes (HLM) indicate a rapid rate of oxidative metabolism. Under the assay conditions used Cl_{int} values < 65 mL/min/kg in MLM and < 36 mL/min/kg in HLM indicate low rate of metabolism by CYP450 enzymes.

[c] Based upon previous work in our laboratory, an effective efflux ratio (EER) value of > 4 suggests that a compound is a substrate for P-gp, whereas values < 2 suggest the compound is unlikely to be a P-gp substrate. For delivery to the CNS, a drug should ideally have an *in vitro* passive permeability > 150 nm/s and should not be a good P-gp substrate (B to A/A to B ratio <2.5).[12]

[d] Poor A to B permeability in both cell types. Low A to B mass balance.

The effect of C1-substitution on potency was investigated initially with compounds comprising the 4-methyl pyrimidin-2-yl capping group (**Table 1**). Methyl and fluoro substitution at C1 (**10** and **12**) conferred an improvement in HDAC4 biochemical activity over trisubstituted cyclopropane **9**, whilst the potency values for the chloro analog **11** and compound **9** were similar. In the cellular HDAC class IIa assay, fluoro derivative **12** exhibited a significant potency enhancement over compounds **9**, **10** and **11**, with no improvement in cellular activity for methyl substituted **10** *versus* **9**. All of the 1-fluoro derivatives (**12**, **14, 16, 18, 20, 22**) demonstrated a consistent positive effect on biochemical and cell activities when compared to the trisubstituted cyclopropanes (**9, 13, 15, 17, 19, 21**).

The opposite enantiomer of **14**, prepared *via* the synthetic route in **Scheme 1** (*vide infra*), was 40-fold less potent in the HDAC4 biochemical and cell assays (compound **26**, see Supporting Information).

The tetrasubstituted cyclopropanes were assessed for *in vitro* ADME properties (**Table 1**). As an indication of oxidative metabolism, compounds **16** and **22** were more stable in mouse liver microsomes (Cl_{int} values of <65 and <67 mL/min/kg BW) than **14** (306 mL/min/kg BW). A mouse microsomal preparation incubated with compound **14** showed the presence of a metabolite that was assigned as the 5-hydroxypyrimidin-2-yl derivative, which may, at least in part, account for the increased microsomal turnover compared to **16** or **22**. Compound **18** was moderately stable in mouse liver microsomes but showed poor solubility and poor passive permeability in MDCK monolayers, whilst **20** also exhibited low passive permeability.

In mouse hepatocytes, all compounds exhibited high intrinsic clearance values (data not shown).

C1-substitution of **9** with either fluorine, chlorine or a methyl group retained the low P-gp efflux (measured in MDR1-MDCK cell monolayers) characteristic of the parent trisubstituted cyclopropanes, with moderate to good passive permeability across wild type MDCK cells. The methyl analog **10** also displayed some improvement in mouse microsomal stability.

A direct measure of compound binding to the target was determined by surface plasmon resonance (SPR) where the HDAC4 catalytic domain was immobilized *via* amine coupling to the sensor surface (see Supporting Information). At steady state, the K_D for compound **14** was determined to be 0.011 μM (**Table 2**), with a K_{on} of 196800 /M.s and a K_{off} of 0.0044 /s, *i.e.* moderate on and off rates. The corresponding *des*-fluoro compound **13** displayed lower affinity, consistent with the biochemical assay, with a K_D value of 0.118 μM, driven by larger K_{off} of 0.0186 /s (the K_{on} value was 190270 /M.s).

Table 2. Comparison of SPR K_D values with biochemical activity values for compounds 13, 14 and 16.

Entry	Biochemical HDAC4 IC_{50} (μM)[a]	SPR K_D (μM)[a]
13	0.05±0.02	0.11±0.01
14	0.01±0.001	0.02±0.01
16	0.03±0.01	0.08±0.06

[a] Arithmetic mean and standard error of ≥3 measurements.

An X-ray co-crystal structure of **14** with the cdHDAC4 (L728A mutant)[6] was obtained confirming the absolute configuration and demonstrating the key interactions of the hydroxamate molecule with the protein binding site. The binding mode of **14** was similar to that of trisubstituted cyclopropane **13** (**Figure 2B**). Comparison with the class I HDACs (**Figure 2A**, with SAHA) shows the tyrosine residue of the class I HDACs projecting into the region of the selectivity pocket in the class IIa isoforms formed by the tyrosine-histidine switch.

The previously reported trisubstituted cyclopropanes are selective for the class IIa *versus* class I and IIb HDAC isoforms. HDAC isoform biochemical selectivity was investigated with the Boc-Lys(TFA)-AMC and Boc-Lys(Ac)-AMC substrates (*vide supra*). The potency values against each of the HDAC isoforms for the trisubstituted cyclopropane **13** and its 1-fluoro derivative **14** are shown in **Table 3**.

Compound **14** maintained a good class IIa HDAC selectivity profile, demonstrating, for example, at least 100-fold selectivity over HDACs 1, 2 and 3.

Figure 2. A. X-ray structure of HDAC2 (class I HDAC) with SAHA (4LXZ).[13] B. Protein structure superposition of HDAC4cd X-ray structures with compounds 13 and 14 (PDB codes: 4CBT, 5A2S, respectively). C. Enlarged region of the HDAC4 active site with compound 14. Residue numbering from PDB files.

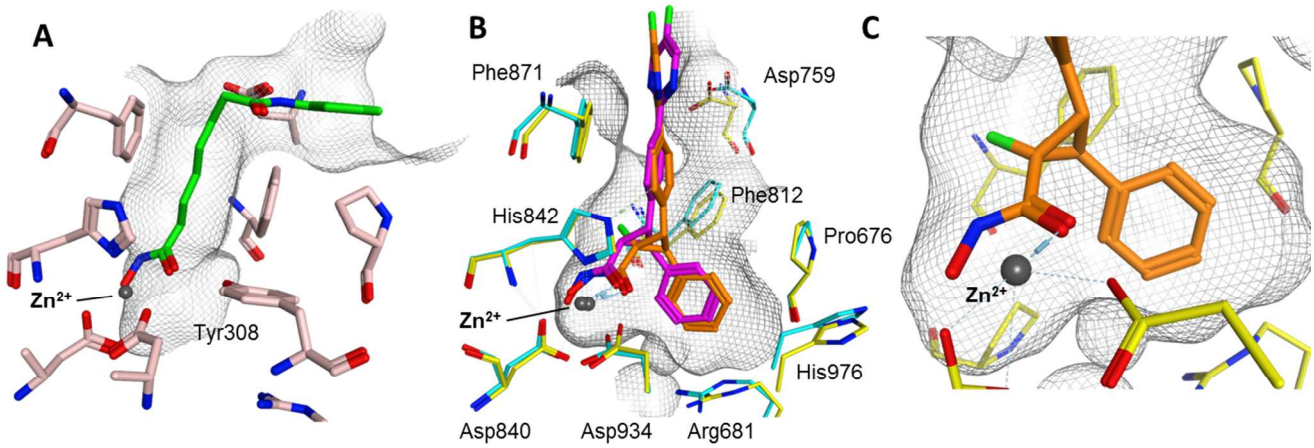

Table 3. HDAC isoform biochemical activity data[a] for compounds 13 and 14.

Entry	Class IIa (cd)				Class I				Class IIb
	HDAC4	HDAC5	HDAC7	HDAC9	HDAC1	HDAC2	HDAC3[b]	HDAC8	HDAC6
13	0.05±0.02	0.03±0.01	0.12±0.06	0.20±0.09	21[c]	ND	9.7±2.2	1.4±0.2	1.9±0.4
14	0.01±0.001	0.01±0.004	0.03±0.01	0.06±0.03	14±4	>50	7.4±2.1	0.28±0.03	3.1±0.4[d]

[a] Inhibition IC_{50} values quoted in μM. Arithmetic mean and standard error of ≥3 measurements; [b] HDAC3-NCoR1; [c] Less than three independent replicates; [d] Determined from a separate assay utilising HDAC6 over-expression in a HEK cell line, due to a lack of availability of active HDAC6 protein. Lysates from these over-expressing cells demonstrated activity that was HDAC6 expression-dependent with only a small background signal due to endogenous HDAC activity.

Compounds **14** and **16** were progressed to *in vivo* PK studies on account of their high potency, MDCK data, and kinetic solubility. At the time of writing, compound **22** had not yet been advanced to further studies.

Trisubstituted cyclopropane **13**, and fluoro cyclopropanes **14** and **16** were dosed intravenously and *via* oral gavage in fed male C57Bl/6 mice. Following an oral dose, all three compounds were rapidly absorbed (**Figure 3**).

Compounds **14** and **16**, incorporating fluoro- or difluoromethoxy pyrimidine capping group substituents respectively, demonstrated higher distribution to brain tissue *versus* the trisubstituted cyclopropane **13**. All three compounds exhibited biphasic elimination profiles and high oral bioavailability (**Table 4**). In addition to high volumes of distribution, these compounds displayed high plasma clearance, as expected from the mouse hepatocyte data. Following oral dosing, a broad secondary peak was observed for **14** and **16**. This may be a result of slow dissolution of compound following gavage.

Compound **14** demonstrated a linear increase in exposure with dose in both plasma and brain matrices across 10, 30 and 100 mg/kg oral doses.

Figure 3. Mouse plasma and brain pharmacokinetic profiles for compounds 13, 14 and 16 post oral dose (10 mg/kg).

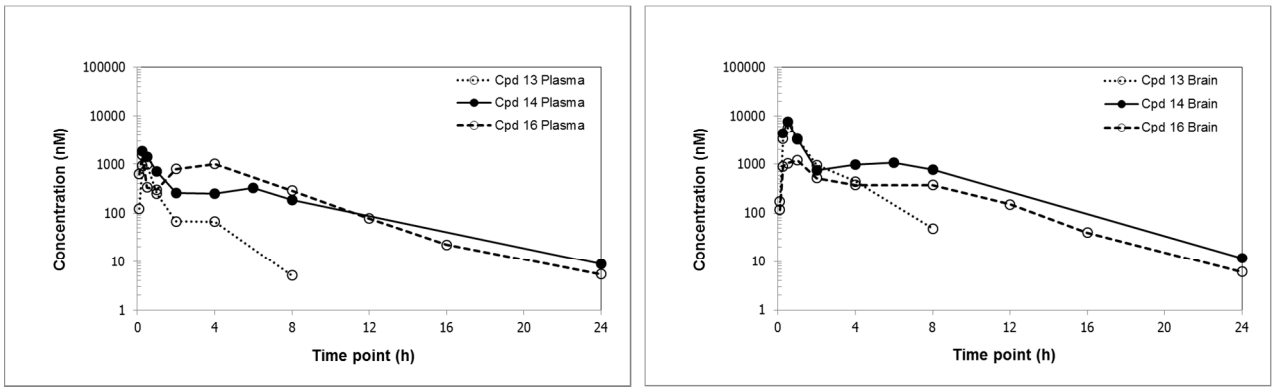

Table 4. Pharmacokinetic parameters of 13, 14 and 16 following administration to fed male C57Bl/6 mice.

		po[a]					*iv*[b]	
Entry	Compartment	F (%)	AUC_{norm} (nM.h.kg/mg)	$C_{max\ norm}$ (nM.kg/mg)	t_{max} (h)	Cl_p (L/h/kg)	Vd_{ss} (L/kg)	$t_{½}$ (h)
13	Plasma	~100[c]	110[d]	97	0.5	11	4.1	0.3
	Brain	ND	830	570	0.5	ND	ND	ND
	Muscle	ND	330	320	0.5	ND	ND	ND
14	Plasma	79	480	180	0.25	4.5	5.1	2.2
	Brain	ND	1900	780	0.5	ND	ND	ND
	Muscle	ND	640	290	0.5	ND	ND	ND
16	Plasma	~100	660	150	0.25	4.4	10	3
	Brain	ND	580	120	1	ND	ND	ND
	Muscle	ND	300	56	0.5	ND	ND	ND

[a]**13**, **14**, & **16** dosed at 10 mg/kg. [b]**13**, **14**, & **16** dosed at 5 mg/kg, 1 mg/kg and 2.5 mg/kg respectively. [c]Oral bioavailability may be underestimated for the 10 mg/kg *po* dose; $AUC_{po} = AUC_{0\text{-}24\ h}$ whilst AUC_{iv} was extrapolated to infinity. [d]Calculated using AUC_{last}.

From HDAC4 SPR studies (*vide supra*) the dissociation half-life for compound **14** is approximately 160 s, considerably shorter than its *in vivo* half-life of ~ 2 h. Binding kinetics are therefore unlikely to impact the duration of any pharmacodynamic effect of **14**.

In the absence of known intracellular concentrations of compound in the brain, we considered that the best estimate of compound available to interact with the target is likely to be the unbound fraction of compound that may be determined either by microdialysis, CSF exposure, or correction of the total exposure from *in vitro* equilibrium dialysis.

Unbound brain concentrations of **14** were estimated by correcting total brain concentrations for the fraction unbound (0.41%) determined in mouse brain homogenate by equilibrium dialysis. CSF concentrations in mouse were estimated using the CSF to brain ratio determined in rat, assuming this remained constant across species. These gave very similar estimates of concentration over the time points (at 10 mg/kg *po* dose the C_{max} measured in rat CSF was at approximately the cell IC_{50} value).

Compounds were synthesized according to **Scheme 1**. Cyclopropanation of the methyl cinnamate derived from **1** as previously described,[6] followed by deprotonation of the racemic intermediate **2** using LDA (1.1-3 eq) and quenching with an appropriate electrophile (MeI, CCl_4 or NFSI)[14] afforded the tetrasubstituted cyclopropane. The desired isomer was isolated by flash chromatography. The heterocyclic capping groups were introduced by Suzuki coupling and the enantiopure hydroxamic acid products were obtained from chiral HPLC purification.

Scheme 1. Synthesis of 1-substituted cyclopropanes and alternative route towards compound 14.

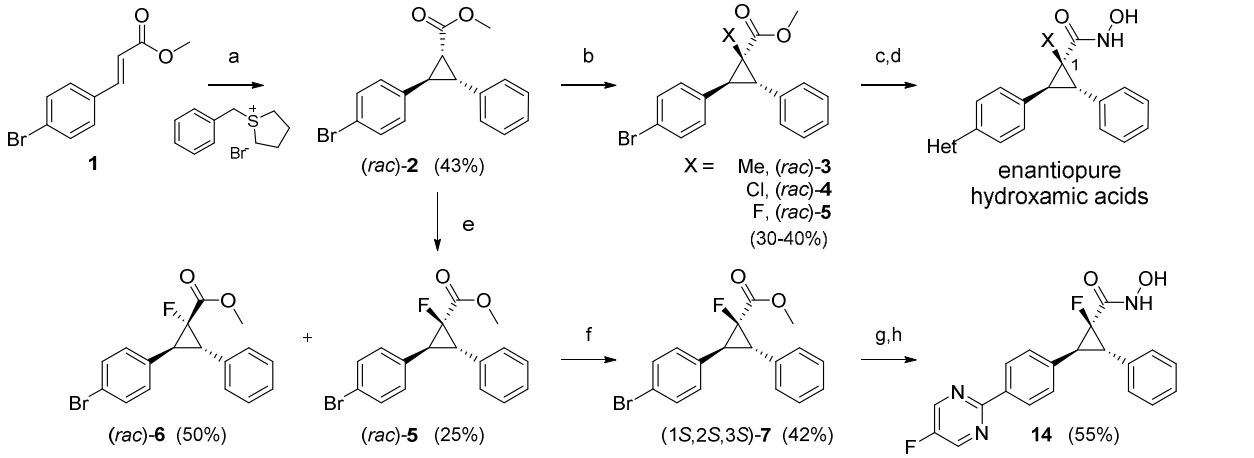

Reagents and conditions: (a) 12-crown-4, LiHMDS, DCM, -20 °C, 1 h; (b) LDA in THF, -78°C, 30 min then MeI or CCl_4 or NFSI, 2 h; (c) (i) *bis*(pinacolato)diboron, KOAc, $Pd(dppf)Cl_2$, dioxane, 90 °C, 4 h; (ii) heteroaryl halide, $Pd(dppf)Cl_2$, CsF, dioxane, 100 °C, 17 h; (d) NH_2OH 50% aq, KOH, THF:MeOH (1:1), r.t., 16 h, chiral HPLC; (e) LDA in THF, -78°C, 30 min then NFSI, 2 h, (*rac*)-**5** separated by flash chromatography; (f) SFC chiral chromatography; (g) (i) *bis*(pinacolato)-diboron, KOAc, $Pd(dppf)Cl_2$, dioxane, 90 °C, 4 h; (ii) 2-chloro-5-fluoropyrimidine, $Pd(dppf)Cl_2$, CsF, dioxane, 100 °C, 17 h; (h) NH_2OH 50% aq, KOH, THF:MeOH (1:1), r.t., 16 h.

In order to access larger quantities of 1-fluoro cyclopropane **14**, a modification of the general route was employed (**Scheme 1**, lower branch). Herein, the bromophenyl fluoro precursor (**7**) was obtained as the single desired stereoisomer. After the key electrophilic fluorination reaction of the cyclopropane ester (*rac*)-**2**, a 1:2 diastereomeric ratio of epimers (*rac*)-**5** and (*rac*)-**6** respectively was achieved using THF and LDA (3 eq.) at -78 °C with NFSI (*N*-fluorobenzene sulfonimide), on a multi-gram scale. This resulted in a 25% isolated yield of (*rac*)-**5** following separation by flash chromatography. The addition of LiCl, previously reported to increase the yields of 1-fluorination of cyclopropyl esters,[15] was discovered to favor further the formation of the undesired diastereoisomer (*rac*)-**6**. The enantiomerically pure methyl ester **7** was isolated by chiral supercritical fluid chromatography (SFC). Subsequently the heterocyclic capping group was introduced by Suzuki coupling, followed by hydroxamic acid formation to deliver compound **14**.

In conclusion, we have discovered potent and selective class IIa HDAC hydroxamic acid inhibitors comprising a tetrasubstituted cyclopropane scaffold. Compounds such as **14** displayed high oral bioavailability with good brain and muscle exposure. Such compounds exhibit suitable properties for assessment of the impact of class IIa HDAC catalytic site inhibition in preclinical HD disease models.

ASSOCIATED CONTENT

Supporting Information. The Supporting Information is available free of charge on the ACS Publications website at DOI: XXXXXXX.

Additional compound data; synthesis procedures and characterization of compounds, quantification of compound binding to HDAC4cd using SPR; X-ray crystallography data collection and refinement statistics; rat pharmacokinetics.

AUTHOR INFORMATION

Corresponding Author

*E-mail: Celia.Dominguez@CHDIFoundation.org. Phone: +1 310-342-5503.

Author Contributions

The manuscript was written through contributions of all authors. All authors have given approval to the final version of the manuscript.

Notes

The authors declare no conflicts of interest.

ACKNOWLEDGMENTS

The authors thank Vahri Beaumont, Ignacio Munoz-Sanjuan, and Michel Maillard (CHDI) for helpful discussions. The authors also express their gratitude to the analytical chemistry and purification team (BioFocus), including Mark Sandle, Nicholas Richards and Paul Bond, and also Tania Mead and Catherine O'Connell for ADME assays.

ABBREVIATIONS

SAHA, suberoylanilide hydroxamic acid; cd, catalytic domain; ND, not determined; *po*, *per os*, oral administration; *iv*, intravenous route of administration; CSF, cerebrospinal fluid.

REFERENCES

(1) Martin, M.; Kettmann, R.; Dequiedt, F. Class IIa histone deacetylases: regulating the regulators. *Oncogene* **2007,** *26*, 5450-5467.

(2) Bertos, N. R.; Wang, A. H.; Yang, X. J. Class II histone deacetylases: structure, function, and regulation. *Biochem. Cell. Biol.* **2001,** *79*, 243-252.

(3) Mielcarek, M.; Benn, C. L.; Franklin, S. A.; Smith, D. L.; Woodman, B.; Marks, P. A.; Bates, G. P. SAHA decreases HDAC2 and 4 levels *in vivo* and improves molecular phenotypes in the R6/2 mouse model of Huntington's disease. *PLoS One* **2011**, *6*, e27746.

(4) Mielcarek, M.; Landles, C.; Weiss, A.; Bradaia, A.; Seredenina, T.; Inuabasi, L.; Osborne, G. F.; Wadel, K.; Touller, C.; Butler, R.; Robertson, J.; Franklin, S. A.; Smith, D. L.; Park, L.; Marks, P. A.; Wanker, E. E.; Olson, E. N.; Luthi-Carter, R.; van der Putten, H.; Beaumont, V.; Bates, G. P. HDAC4 reduction: a novel therapeutic strategy to target cytoplasmic huntingtin and ameliorate neurodegeneration. *PLoS Biol.* **2013**, *11*, e1001717.

(5) Mielcarek, M.; Zielonka, D.; Carnemolla, A.; Marcinkowski, J. T.; Guidez, F. HDAC4 as a potential therapeutic target in neurodegenerative diseases: a summary of recent achievements. *Front. Cell. Neurosci.*, published online March 23, 2009: DOI: 10.3389/fncel.2015.00042.

(6) Bürli, R. W.; Luckhurst, C. A.; Aziz, O.; Matthews, K. L.; Yates, D.; Lyons, K. A.; Beconi, M.; McAllister, G.; Breccia, P.; Stott, A. J.; Penrose, S. D.; Wall, M.; Lamers, M.; Leonard, P.; Muller, I.; Richardson, C. M.; Jarvis, R.; Stones, L.; Hughes, S.; Wishart, G.; Haughan, A. F.; O'Connell, C.; Mead, T.; McNeil, H.; Vann, J.; Mangette, J.; Maillard, M.; Beaumont, V.; Munoz-Sanjuan, I.; Dominguez, C. Design, synthesis, and biological evaluation of potent and selective class IIa histone deacetylase (HDAC) inhibitors as a potential therapy for Huntington's disease. *J. Med. Chem.* **2013**, *56*, 9934-9954.

(7) Lahm, A.; Paolini, C.; Pallaoro, M.; Nardi, M. C.; Jones, P.; Neddermann, P.; Sambucini, S.; Bottomley, M. J.; Lo Surdo, P.; Carfí, A.; Koch, U.; De Francesco, R.; Steinkühler, C.; Gallinari, P. Unraveling the hidden catalytic activity of vertebrate class IIa histone deacetylases. *Proc. Natl. Acad. Sci. U.SA.* **2007**, *104*, 17335-17340.

(8) Bottomley, M J ; Lo Surdo, P.; Di Giovine, P.; Cirillo, A.; Scarpelli, R.; Ferrigno, F.; Jones, P.; Neddermann, P.; De Francesco, R.; Steinkühler, C.; Gallinari, P.; Carfí, A. Structural and functional analysis of the human HDAC4 catalytic domain reveals a regulatory structural zinc-binding domain. *J. Biol. Chem.* **2008**, *283*, 26694-26704.

(9) Beconi, M.; Aziz, O.; Matthews, K.; Moumne, L.; O'Connell, C.; Yates, D.; Clifton, S.; Pett, H.; Vann, J.; Crowley, L.; Haughan, A. F.; Smith, D. L.; Woodman, B.; Bates, G. P.; Brookfield, F.; Bürli, R. W.; McAllister, G.; Dominguez, C.; Munoz-Sanjuan, I.; Beaumont, V. Oral administration of the pimelic diphenylamide HDAC inhibitor HDACi *4b* is unsuitable for chronic inhibition of HDAC activity in the CNS *in vivo*. *PLoS One* **2012,** *7*, e44498.

(10) Bradner, J. E.; West, N.; Grachan, M. L.; Greenberg, E. F.; Haggarty, S. J.; Warnow, T.; Mazitschek, R. Chemical phylogenetics of histone deacetylases. *Nat. Chem. Biol.* **2010**, *6*, 238-243.

(11) Bradner, J. E. Fluorinated HDAC inhibitors and uses thereof, *WO20110849911*.

(12) Mahar Doan, K. M.; Humphreys, J. E.; Webster, L. O.; Wring, S. A.; Shampine, L. J.; Serabjit-Singh, C. J.; Adkinson, K. K.; Polli, J. W. Passive permeability and P-glycoprotein-

mediated efflux differentiate central nervous system (CNS) and non-CNS marketed drugs. *J. Pharm. Exp. Ther.* **2002**, *303*, 1029-1037.

(13) Lauffer, B. E.; Mintzer, R.; Fong, R.; Mukund, S.; Tam, C.; Zilberleyb, I.; Flicke, B.; Ritscher, A.; Fedorowicz, G.; Vallero, R.; Ortwine, D. F.; Gunzner, J.; Modrusan, Z.; Neumann, L.; Koth, C. M.; Lupardus, P. J.; Kaminker, J. S.; Heise, C. E.; Steiner, P. Histone deacetylase (HDAC) inhibitor kinetic rate constants correlate with cellular histone acetylation but not transcription and cell viability. *J. Biol. Chem.* **2013**, *288*, 26926-26943.

(14) Feit, B. A.; Elser, R.; Melamed, U.; Goldberg, I. Cyclopropyl carbanions derived from esters of 2-phenylcyclopropanecarboxylic acids: configurational stability and reaction with electrophiles. *Tetrahedron* **1984**, *40*, 5177-5180.

(15) Zhou, S.; Kern, E. R.; Gullen, E.; Cheng, Y-C.; Drach, J. C.; Matsumi, S.; Mitsuya, H.; Zemlicka, J. (*Z*)- and (*E*)-[2-Fluoro-2-(hydroxymethyl)cyclopropylidene]methylpurines and pyrimidines, a new class of methylenecyclopropane analogs of nucleosides: synthesis and antiviral activity. *J. Med. Chem.* **2004**, *47*, 6964-6972.

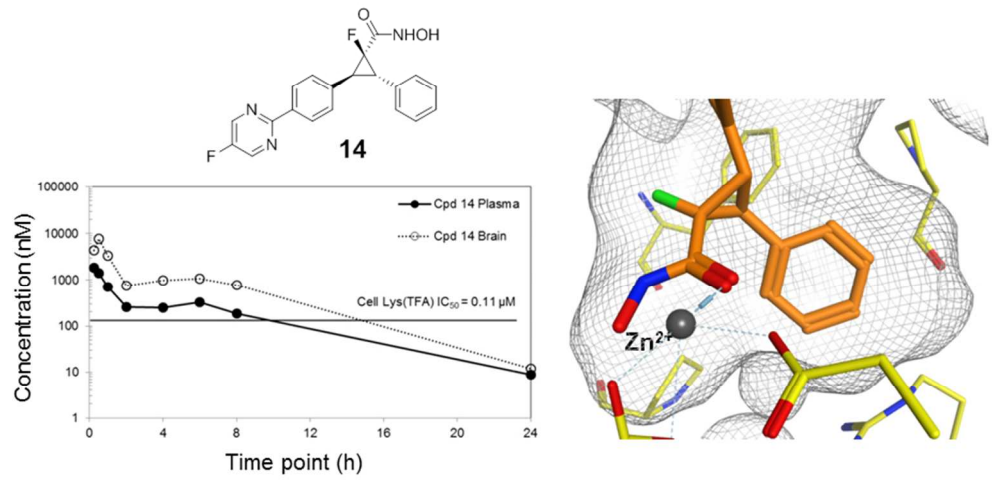

157x79mm (150 x 150 DPI)